Calibration and validation of FengYun satellites thermal infrared channels using unmanned surface vehicle at CRCS Lake Qinghai

Presented by Yong Zhang[1]

Contributors: Lijun Zhang[1], Yidan Si[1], Dongyu Duan[1], Yonghong Hu[2], Lin Yan[2], Hongbin Chen[3], Yu Zhao[3], Wenzheng Wang[3], Xiaopeng Hao[4], Zundong Yuan[4]

1. National Satellite Meteorologic Center, China Meteorological Administration
2. Aerospace Information Research Institute, Chinese Academy of Sciences
3. Institute of Atmospheric Physics, Chinese Academy of Sciences
4. National Institute of Metrology, China

Outline

- Background and motivation
- Satellite data analysis
- USV data processing
- Atmospheric parameters processing
- Radiative transfer simulation
- Calibration and validation results
- Preliminary results of CRCS Lake Qinghai 2021

FengYun satellites have launched 19 since 1988

China Radiometric Calibration Sites (CRCS)

Lake Qinghai Site: Lake Qinghai is the largest saline of China and located in the northeast of Tibet Plateau. Lake Qinghai (36°45N, 100°20E) is located 150km from Xining City, capital of Qinghai Province. Its total area is 4473 km^2 and the perimeter is 360km The elevation of the water surface is 3196 m and the cubage of the lake is 105 Gm^3. It is a good place for IR bands' calibrating.

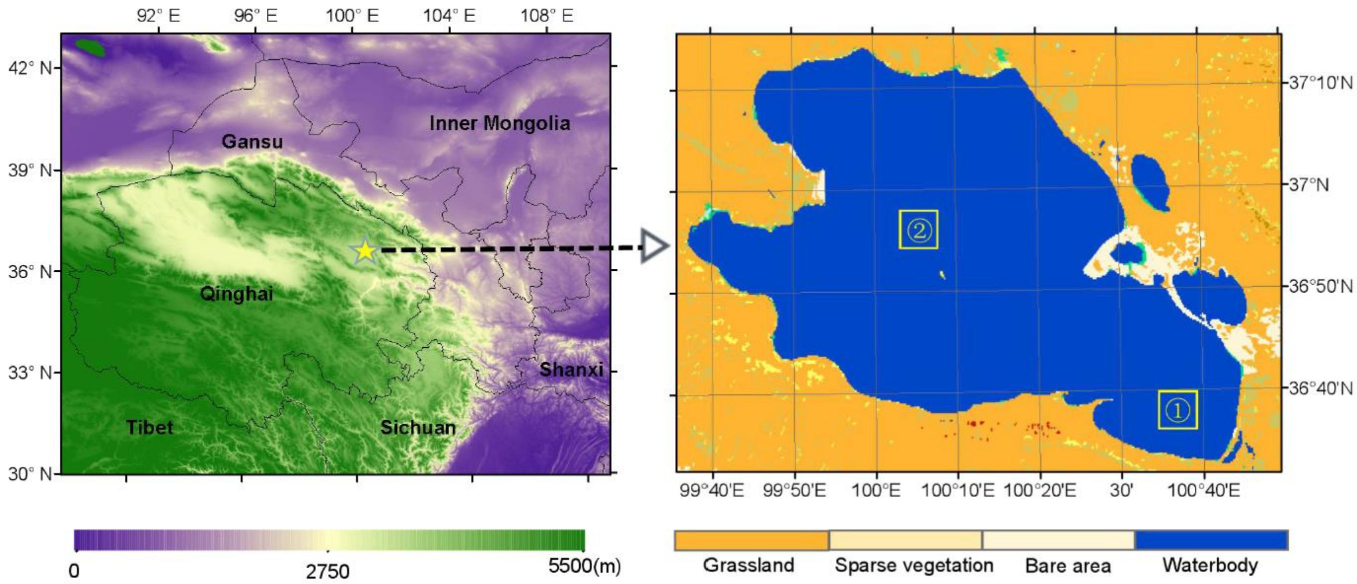

Fig. 1. Location, (Left) altitude, and (Right) surrounding environment of Lake Qinghai. The data were collected from the SRTM DEM and ESA-CCI land cover product in 2015. The marked square 1 in right is the location of the field experiment, and square 2 is the location for selecting clear sky pixels from satellite images when square 1 is influenced by cloud cover.

Using CRCS Lake Qinghai to validate and evaluate onboard calibration accuracy.

CRCS Lake Qinghai field campaign 2019

Changes in the way of measuring on the lake

- Reduce labor and financial costs
- Ensure the safety of personnel

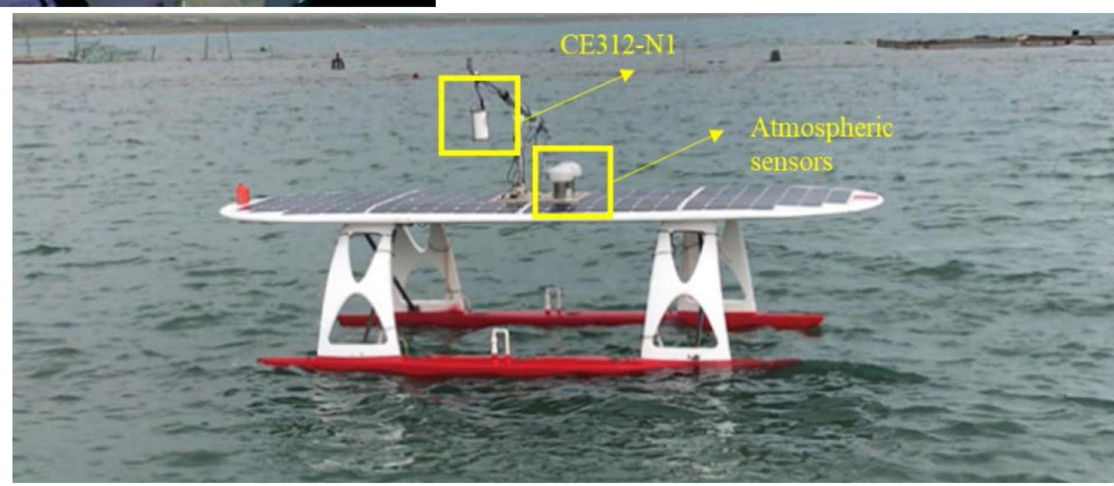

FY-3D MERSI and FY-4A AGRI

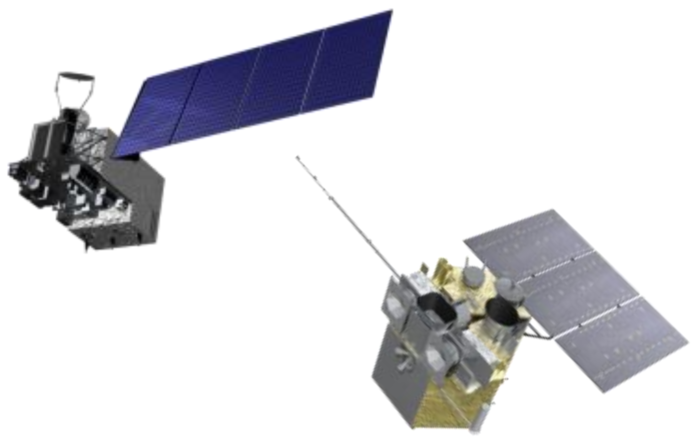

Table 1. Specifications of the Fengyun 3D Advanced Medium Resolution Spectral Imager (FY3D MERSI-II).

Band Number	Center Wave-length (μm)	Bandwidth (nm)	Spatial Resolu-tion (m)	SNR or NEΔT (K)	Maximum Reflectance ρ or Dynamic Range (K)
1	0.47	50	250	100	90%
2	0.55	50	250	100	90%
3	0.65	50	250	100	90%
4	0.865	50	250	100	90%
5	1.38	20/30	1000	60/100	90%
6	1.64	50	1000	200	90%
7	2.13	50	1000	100	90%
8	0.412	20	1000	300	30%
9	0.443	20	1000	300	30%
10	0.49	20	1000	300	30%
11	0.555	20	1000	500	30%
12	0.67	20	1000	500	30%
13	0.709	20	1000	500	30%
14	0.746	20	1000	500	30%
15	0.865	20	1000	500	30%
16	0.905	20	1000	200	100%
17	0.936	20	1000	100	100%
18	0.940	50	1000	200	100%
19	1.030	20	1000	100	100%
20	3.800	180	1000	0.25 K	200–350 K
21	4.050	155	1000	0.25 K	200–350 K
22	7.200	500	1000	0.30 K	200–350 K
23	8.550	300	1000	0.25 K	200–350 K
24	10.800	1000	250	0.40 K	200–350 K
25	12.000	1000	250	0.40 K	200–350 K

TABLE I

SPECTRAL AND SPATIAL SPECIFICATIONS OF FY-4A AGRI

	Band (μm)	Spatial Resolution(km)	Sensitivity	Main Application
1	0.45～0.49	1	S/N≥90(ρ=100%)	Aerosol
2	0.55～0.75	0.5～1	S/N≥200(ρ=100%)	Fog, Cloud
3	0.75～0.90	1	S/N≥5(ρ=1%)@0.5Km	Vegetation
4	1.36～1.39	2		Cirrus
5	1.58～1.64	2	S/N≥200(ρ=100%)	Cloud,Snow
6	2.1～2.35	2～4		Cirrus,Aerosol
7	3.5～4.0(High)	2	NEΔT≤0.7K(300K)	Fire
8	3.5～4.0(Low)	4	NEΔT≤0.2K(300K)	Land surface
9	5.8～6.7	4	NEΔT≤0.3K(260K)	WV
10	6.9～7.3	4	NEΔT≤0.3K(260K)	WV
11	8.0～9.0	4	NEΔT≤0.2K(300K)	WV,Cloud
12	10.3～11.3	4	NEΔT≤0.2K(300K)	SST
13	11.5～12.5	4	NEΔT≤0.2K(300K)	SST
14	13.2～13.8	4	NEΔT≤0.5K(300K)	CTH

NEΔT = noise equivalent differential temperature, WV = water vapor, SST=sea surface temperature, CTH=cloud top height.

Spectral and spatial specifications

Satellite data analysis

Field campaign period from Aug. 16 to 20, 2019

2019-08-16 14:30
Julian day-228

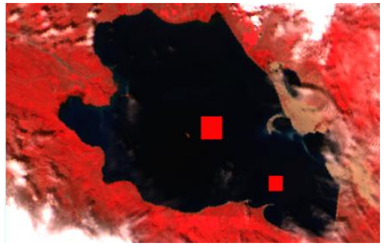

2019-08-17 13:35
Julian day-229

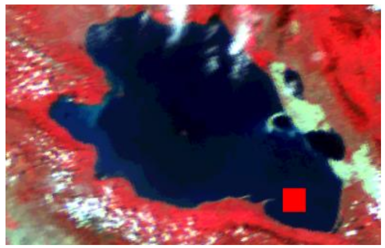

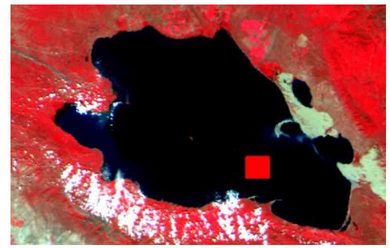

2019-08-17 12:00
Julian day-229

2019-08-18 14:20
Julian day-230

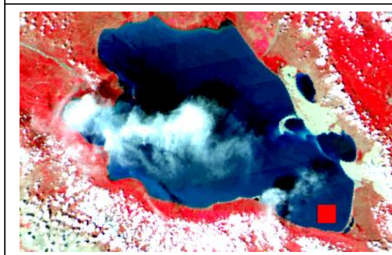

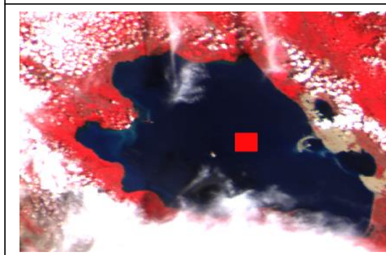

2019-08-18 12:40
Julian day-230

2019-08-19 13:25
Julian day-231

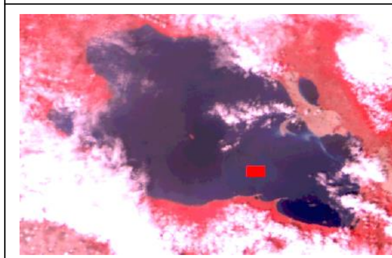

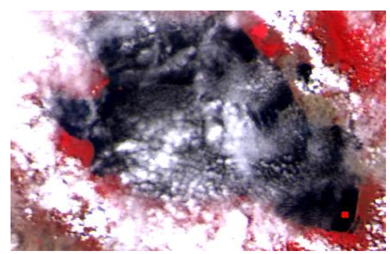

2019-08-19 11:45
Julian day-231

2019-08-20 14:05
Julian day-232

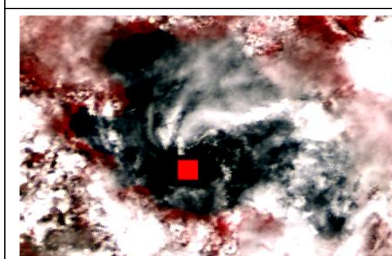

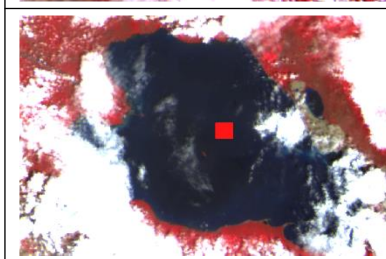

2019-08-20 12:30
Julian day-232

Satellite observing CRCS Lake Qinghai

FY3D image on Aug. 18 at Lake Qinghai

FY3D_MERSI_GBAL_L1_20190818_0630_1000M_MS

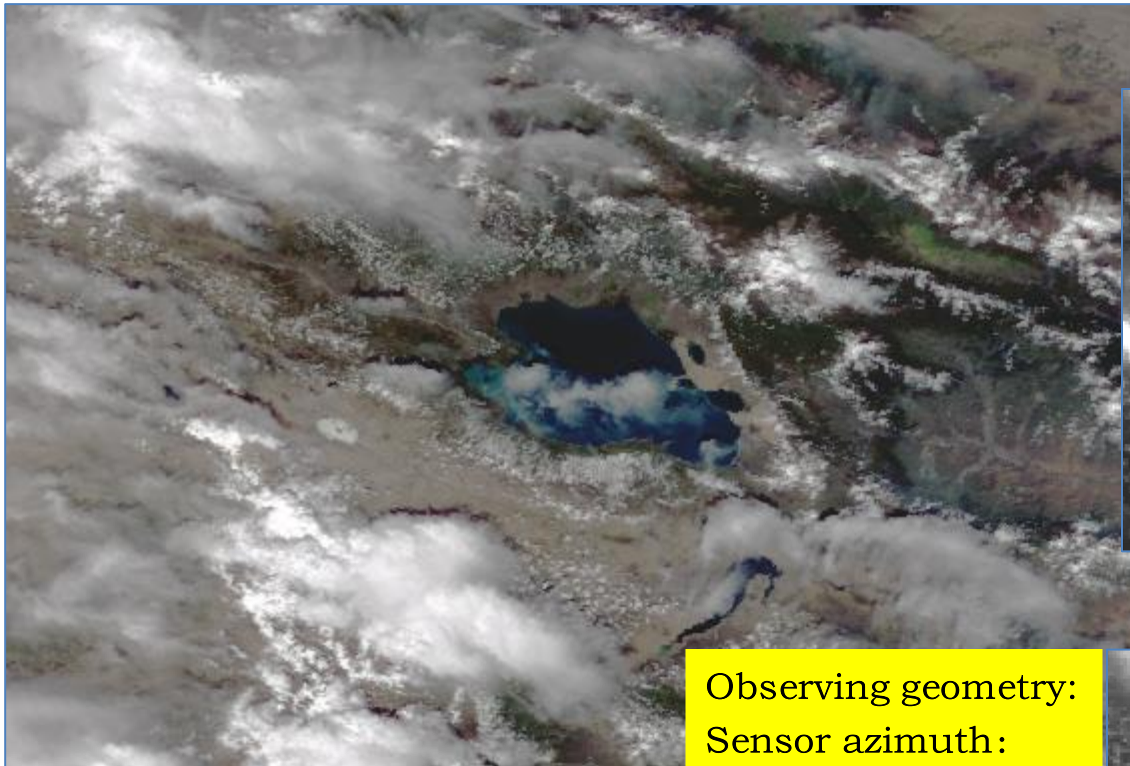

FY3D BAND24

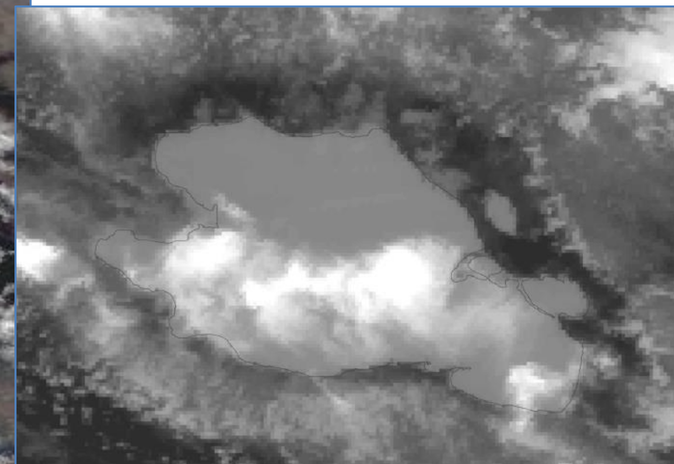

FY3D BAND25

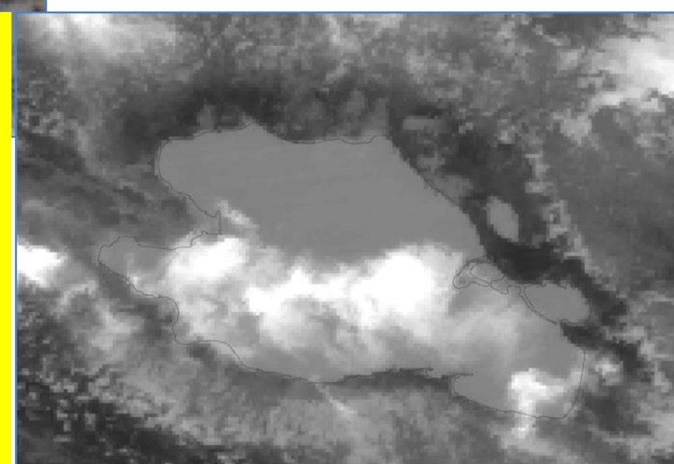

Observing geometry:
Sensor azimuth:
261.50480000
Sensor zenith:
21.33440000
Sun azimuth:
219.20280000
Sun zenith:
28.47040000

FY3D observing time:14:30 (Beijing time)

Differences of lake surface BT in different areas

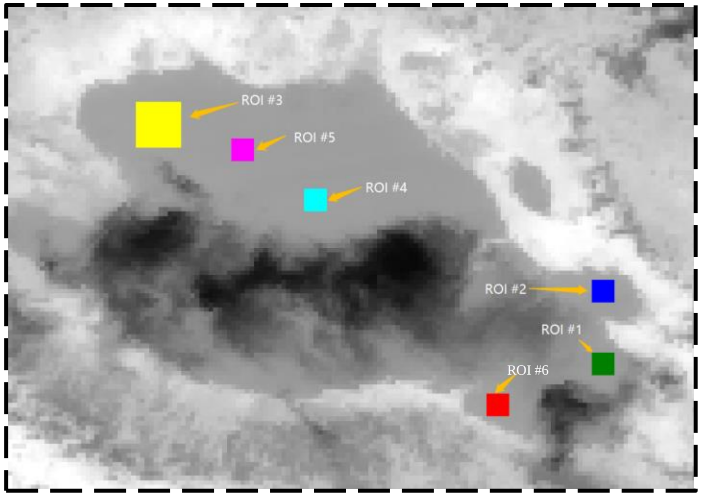

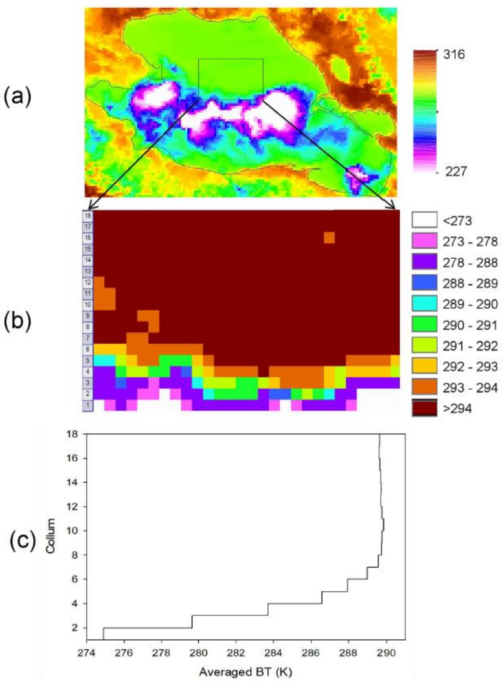

Fig. 8. Influence of cloud cover on satellite-derived at-sensor BT. (a) BT image in Lake Qinghai derived from FY3D-MERSI on August 18 and (b) region close to cloud was selected to identify the extent altered by cloud edge effect. (c) The averaged BT for every columns of the selected region was used to examine the BT change along cloud to lake surface gradient.

MERSI Band #24				
ROI	DN	Stand Deviation	Bright Temperature	Stand Deviation
ROI #1	9243.64	29.464498	289.7364754	0.196894
ROI #2	9499.04	92.131464	291.4301803	0.607283
ROI #3	9470.79	38.923726	291.2441062	0.256782
ROI #4	9366.84	18.814179	290.5567243	0.124831
ROI #5	9370.28	16.634602	290.57954	0.110316
ROI #6	9383.16	52.343163	290.6649247	0.346384

MERSI Band #25				
ROI	DN	Stand Deviation	Bright Temperature	Stand Deviation
ROI #1	10664.4	35.046398	288.9308716	0.225404
ROI #2	10881.88	37.802469	290.3222743	0.240534
ROI #3	10840.2	53.172105	290.0567281	0.339319
ROI #4	10763.64	43.268426	289.5675878	0.277051
ROI #5	10807.4	32.843061	289.8473879	0.209806
ROI #6	10730.2	53.311975	289.3533785	0.341171

TABLE II

SATELLITE IMAGES SELECTED IN REGION 1 AND REGION 2 FOR DERIVING BT DURING RADIOMETRIC CALIBRATION EXPERIMENTS

Overpass	USV location (lon, lat)	Rn	Overpass	USV location (lon, lat)	Rn
13:15, August 18	100.64508, 36.55431	2	12:15, August 20	100.63691, 36.58412	2
13:19, August 18	100.64506, 36.5543	2	12:19, August 20	100.63983, 36.58422	2
13:23, August 18	100.64502, 36.55434	2	12:23, August 20	100.64268, 36.58434	2
13:30, August 18	100.64507, 36.55437	2	12:30, August 20	100.64758, 36.58434	2
13:34, August 18	100.64512, 36.55449	2	12:34, August 20	100.64873, 36.58314	2
13:38, August 18	100.64535, 36.55606	2	12:38, August 18	100.63691, 36.58412	2
14:34, August 18	100.6462, 36.57549	1	12:45, August 20	100.64804, 36.57875	2
14:38, August 18	100.64491, 36.57546	1	12:49, August 20	100.64698, 36.57522	2
14:45, August 18	100.6425, 36.57545	1	12:53, August 18	100.6451, 36.5755	2
14:49, August 18	100.63941, 36.57544	1	13:15, August 20	100.63588, 36.57658	2
14:53, August 18	100.62791, 36.57542	1	13:19, August 20	100.63615, 36.57853	2
			13:23, August 20	100.63635, 36.57996	2
			13:30, August 20	100.63689, 36.584	2
			13:34, August 20	100.64297, 36.58436	2
			13:38, August 20	100.64634, 36.58437	2

Rn: Region number (region 1 or region2 in the lake)
*Local time used here to delineate satellite overpass time

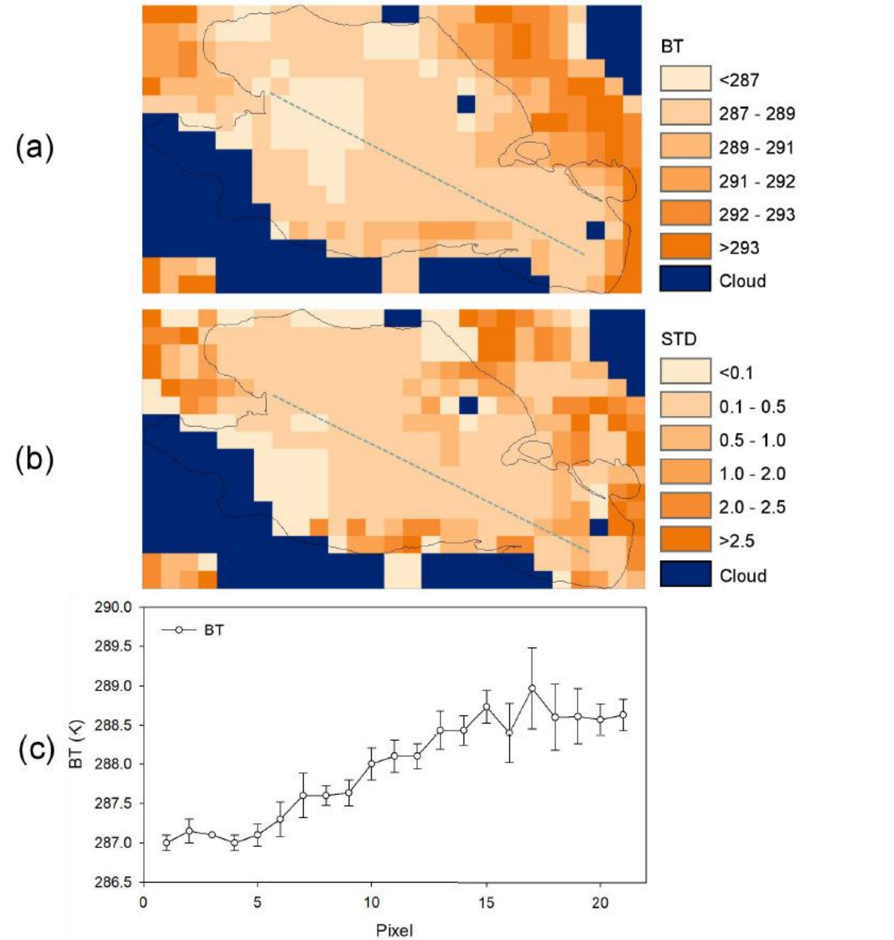

Fig. 5. Distribution of water temperature (K) over the lake surface. The 15 AGRI images were used to derive the (a) averaged temperature and (b) temperature variation during the selected period. In order to examine the details of temperature gradient from west to east in the lake, a transect [dotted line (a) and (b)] was used here to examine (c) water temperature change

Solar Power Unmanned Boat Modification

- In order to meet the requirements of Lake Qinghai satellite-ground synchronous observation field test, the unmanned boat was modified, and the CE312 radiometer was mounted on the boat for water surface observation.

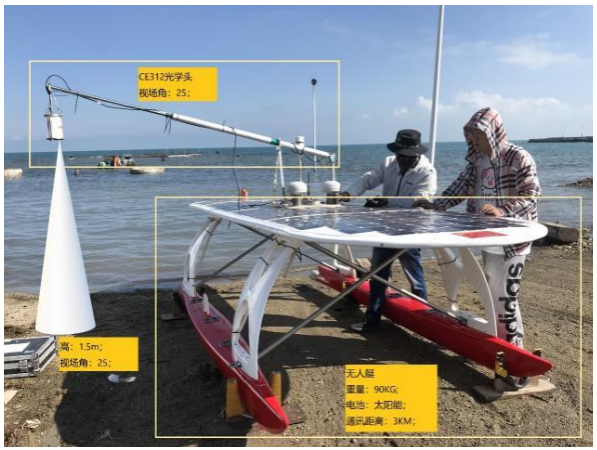

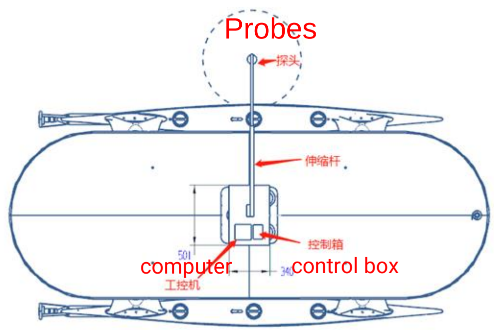

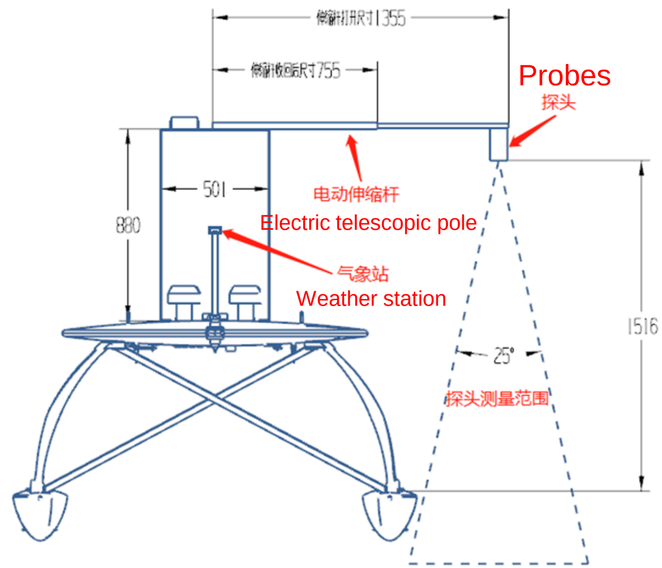

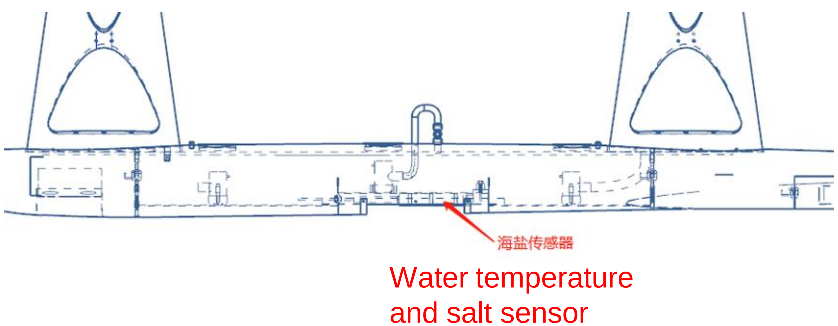

Equipment installation conditions:

1 The height of the equipment from the water surface is not less than 1.5 meters

2 The probe detects no interference within 25°

When in use, the electric telescopic rod extends the straight rod 600mm, the probe performs the measurement, and then returns the collected data to the ground station. After the work is completed, the straight rod is retracted.

NSMC

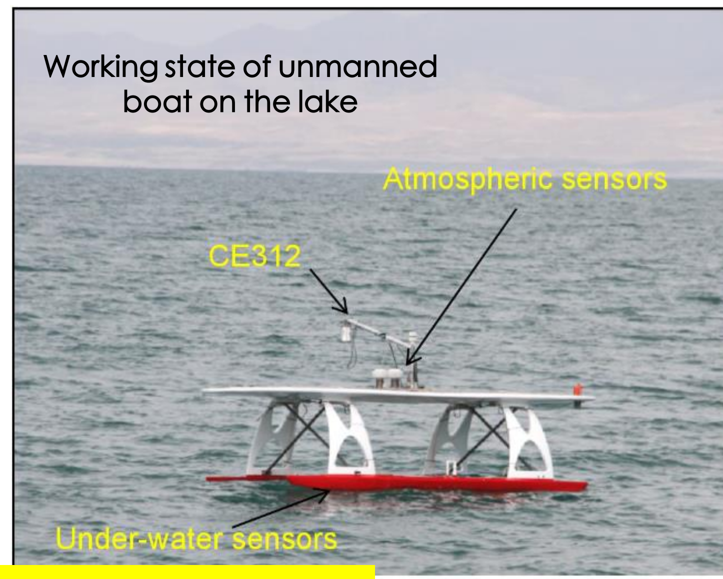

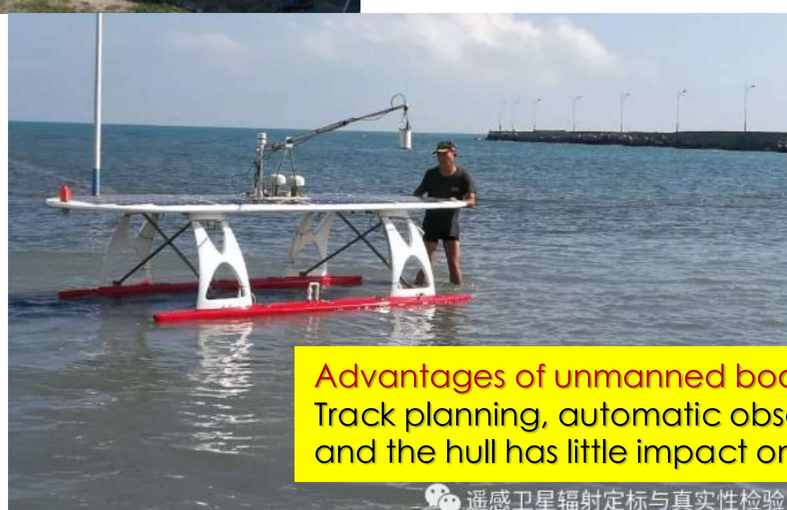

Advantages of unmanned boats:
Track planning, automatic observing, save manpower, and the hull has little impact on the water surface;

Track record of unmanned boat observing 2019-08-18

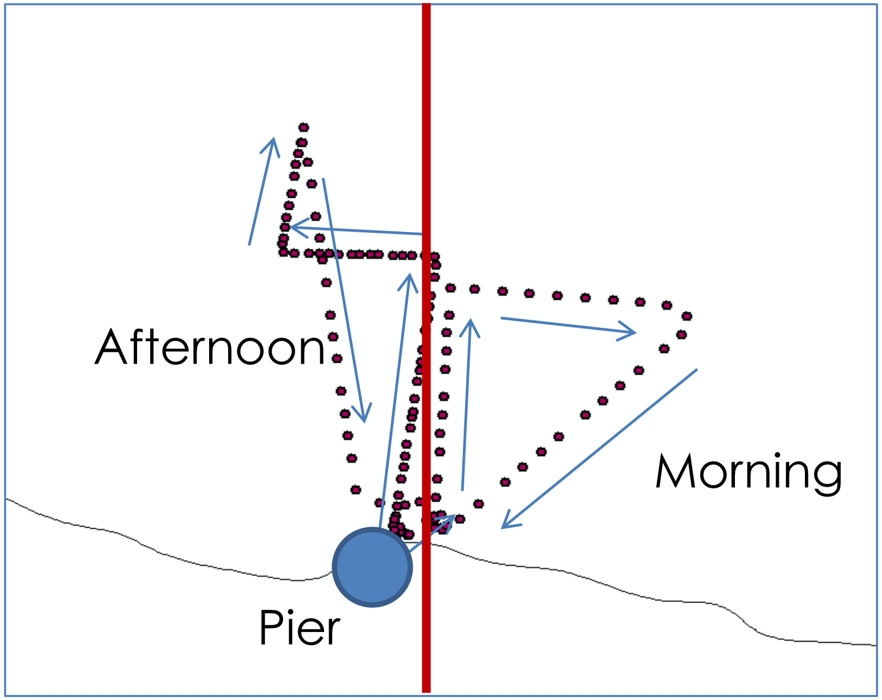

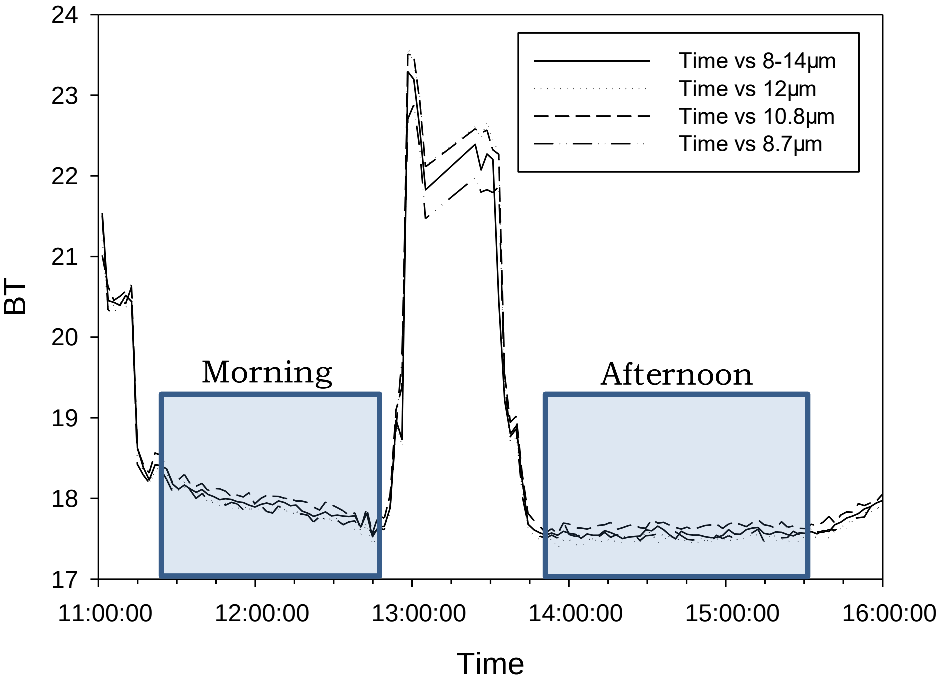

Atmospheric parameters processing

Radiosonde data 2019-08-18~21

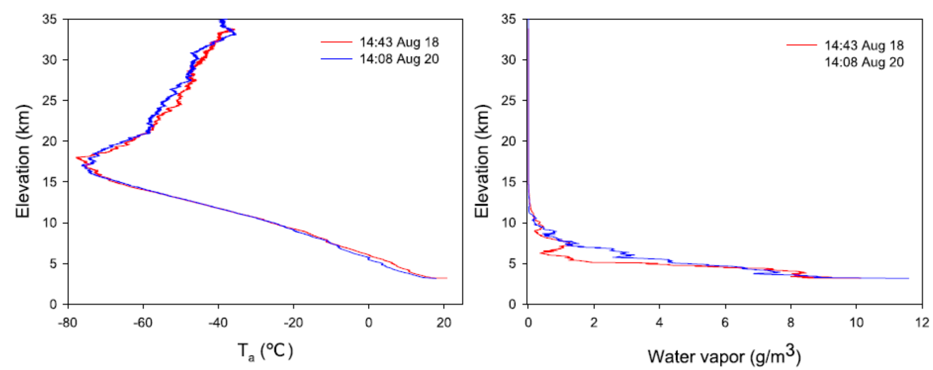

Fig. 6. (Left) Atmospheric temperature and (Right) water vapor profiles measured at calibration site of Lake Qinghai on August 18, 2019, and August 20, 2019.

CE318 sun photometer data processing

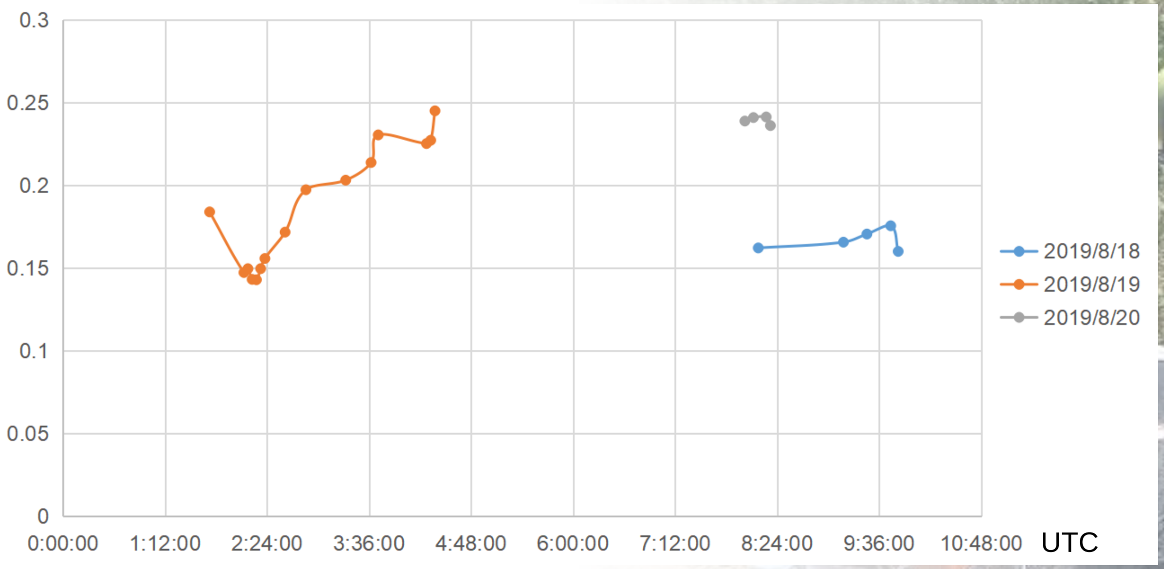

Date	Air mass	1020nm	870nm	670nm	440nm	550nm	β	α
8.18	1.099~2.198	0.0817	0.103	0.104	0.239	0.182	0.0876	1.234
8.19	1.117~1.693	0.0819	0.105	0.105	0.268	0.198	0.0872	1.389
8.20	1.19~1.578	0.192	0.208	0.209	0.285	0.258	0.196	0.464
Mean		0.118	0.138	0.139	0.264	0.213	0.124	1.029

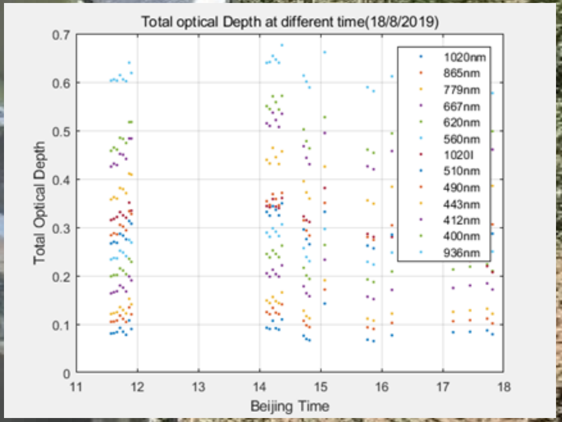

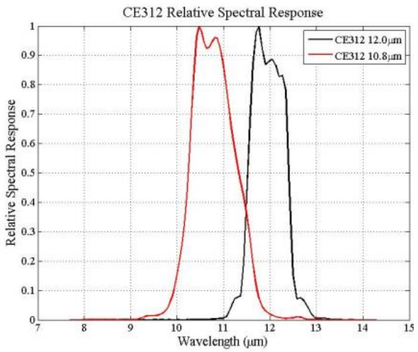

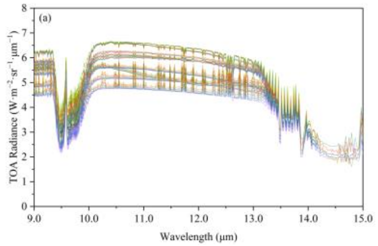

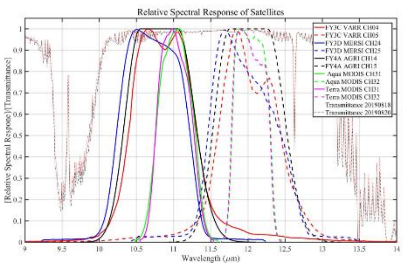

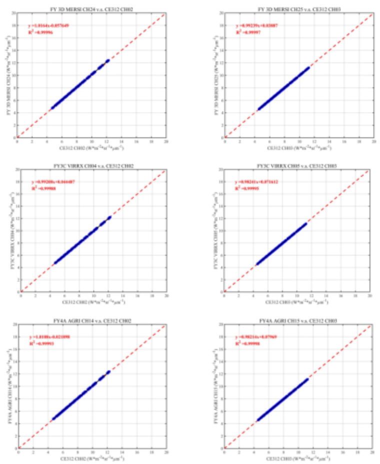

Spectral matching

- Combinations in the MODTRAN simulation were adopted to generate their relative TOA spectral radiance , including 9 different targets (cloud cover, desert, dry grass, field, forest, fresh snow, maple, ocean, and wet grass), 2 satellite view angles (0° and 10°), 6 built-in atmospheric profiles of MODTRAN (Tropical, Mid-latitude Summer/Winter, Sub-Arctic Summer/Winter, U.S. Standard), and 9 boundary temperatures (278 K, 283 K, 288 K, 293 K, 298 K, 303 K, 208 K, 212 K, and 320K).
- The spectral matching were derived from the 972 pairs of unified channel equivalent radiance using linear regression analysis.

Prediction for at-sensor temperature by radiative transfer model

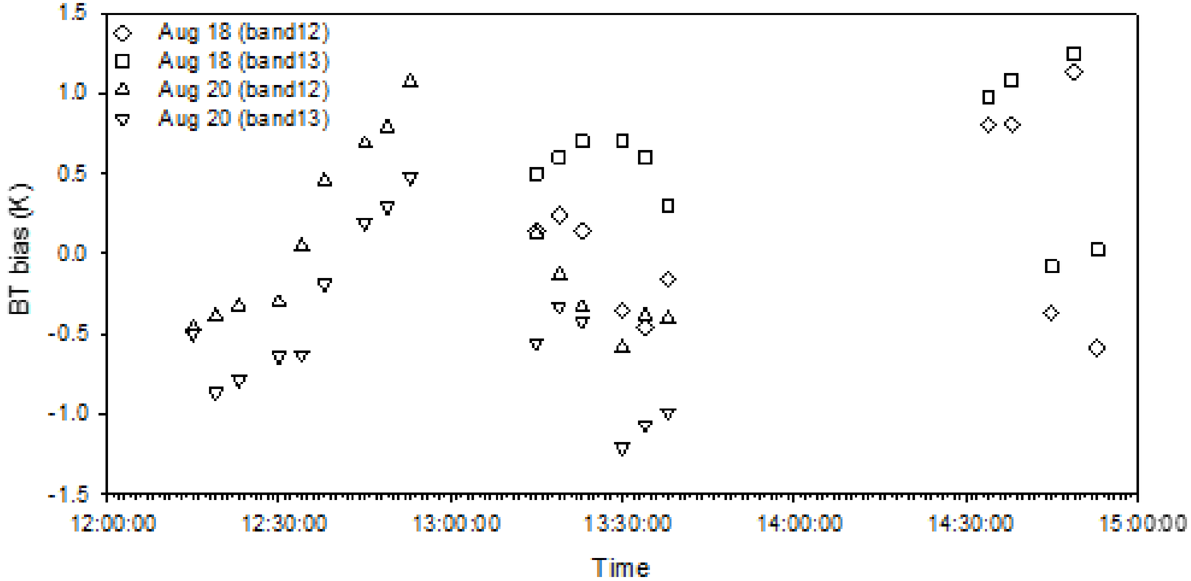

Comparison for the predicted at-sensor brightness temperature and satellite-derived at-senor brightness temperature during the selected period of field campaign. Brightness temperature bias is calculated by using satellite-derived at-sensor BT minus predicted at-sensor BT.

The calibration site with high altitude and dry atmosphere has great advantages in reducing the influence of the atmosphere for ground-based radiometric calibration experiments , and Lake Qinghai is one of the most representative sites with 3196 m elevation. The parameters (surface atmospheric conditions, atmospheric profiles and satellite observation information) were edited and adopted in the Moderate Resolution Atmospheric Transmission Model (MODTRAN 4.0) to derive path radiance and spectral transmittance during propagation process from lake surface to TOA. Then, the simulation results from MODTRAN were convolved with the instrument channel spectral response functions (RSR) to obtain the band-averaged values of the atmospheric parameters. Finally, the at-senor radiance was predicted by reducing the influence of atmospheric absorption and scattering.

Calibration and validation results

- This field campaign investigated the absolute radiometric calibration accuracy of FY4A AGRI and FY3D MERSI thermal infrared band data with field measurement data collected in Lake Qinghai on August 18 and 20, 2019.
- An USV equipped with TIR radiometers was used to continuously collect the water surface skin temperature and surface atmospheric parameters. The atmospheric profiles were measured near calibration experiment site. The atmospheric transfer code was used to simulate path radiance and transmittance propagated from land surface targets to satellite instrument entrance aperture.
- We also proposed a spectral matching method based on atmospheric transfer simulation to eliminate spectral mismatch between CE312 and FY4A AGRI/ FY3D MERSI TIR channels.
- For FY4A AGRI, the calibration accuracy between split-window bands 12 and 13 reached 0.12 K with a RMSE of ±0.17 K and 0.61K with a RMSE of ±0.22 K on August 18 based on exactly concurrent experiment measurements, while it reached -0.01K with a RMSE of ±0.13 K and -0.48K with a RMSE of ±0.17 K on August 20 using satellite at-sensor brightness temperature from replaced measurement region in west part of the lake.
- For FY3D MERSI, the difference between the simulated brightness temperature and satellite brightness temperature is less than -0.346K and -0.722K for channel 24 on August 18 and 20, while it increases to -0.460K and -1.036K for channel 25 on August 18 and 20, respectively.
- Therefore, the absolute radiometric accuracy specified for AGRI and MERSI bands was achieved in AGRI bands 12/13 and MERSI bands 24/25 with calibration error less than 1 K in most cases, which indicates that AGRI and MERSI TIR bands have a good functional status.

Yonghong Hu, Yong Zhang*, Lin Yan, et al. IEEE TGRS, https://doi.org/10.1109/TGRS.2020.3037828.
Yan, L.; Hu, Y.; Zhang, Y*. et al. Remote Sens. 2021, 13, 466. https://doi.org/10.3390/rs13030466

Preliminary results of CRCS Lake Qinghai 2021

- From Sep.16 to 24, field campaign for FY3E and FY4B on-orbit test, calibration and validation for FY3D and FY4A.
- Upgraded unmanned boat equipped with CE312 measuring water surface infrared radiance.
- Added video surveillance on board

Appreciate the help of Hongbin Chen's USV group from the Key Laboratory of Middle Atmosphere and Global Environment Observation (LAGEO), the Institute of Atmospheric Physics, and the Chinese Academy of Sciences.

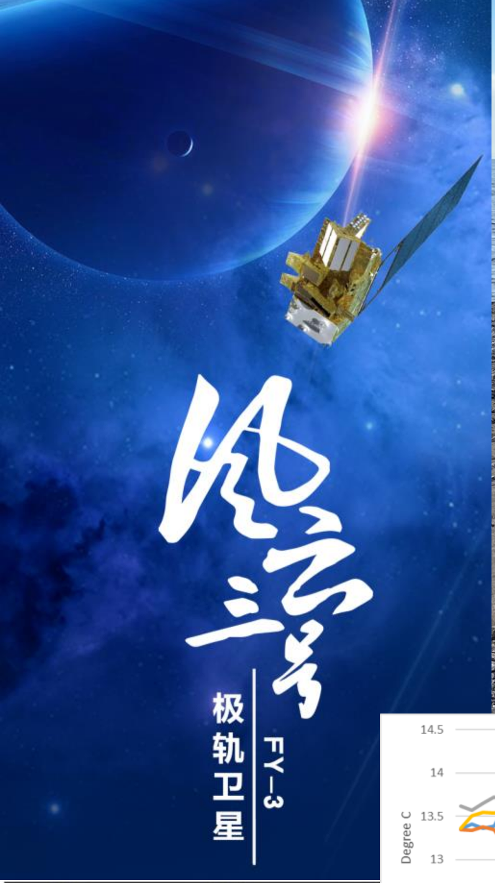

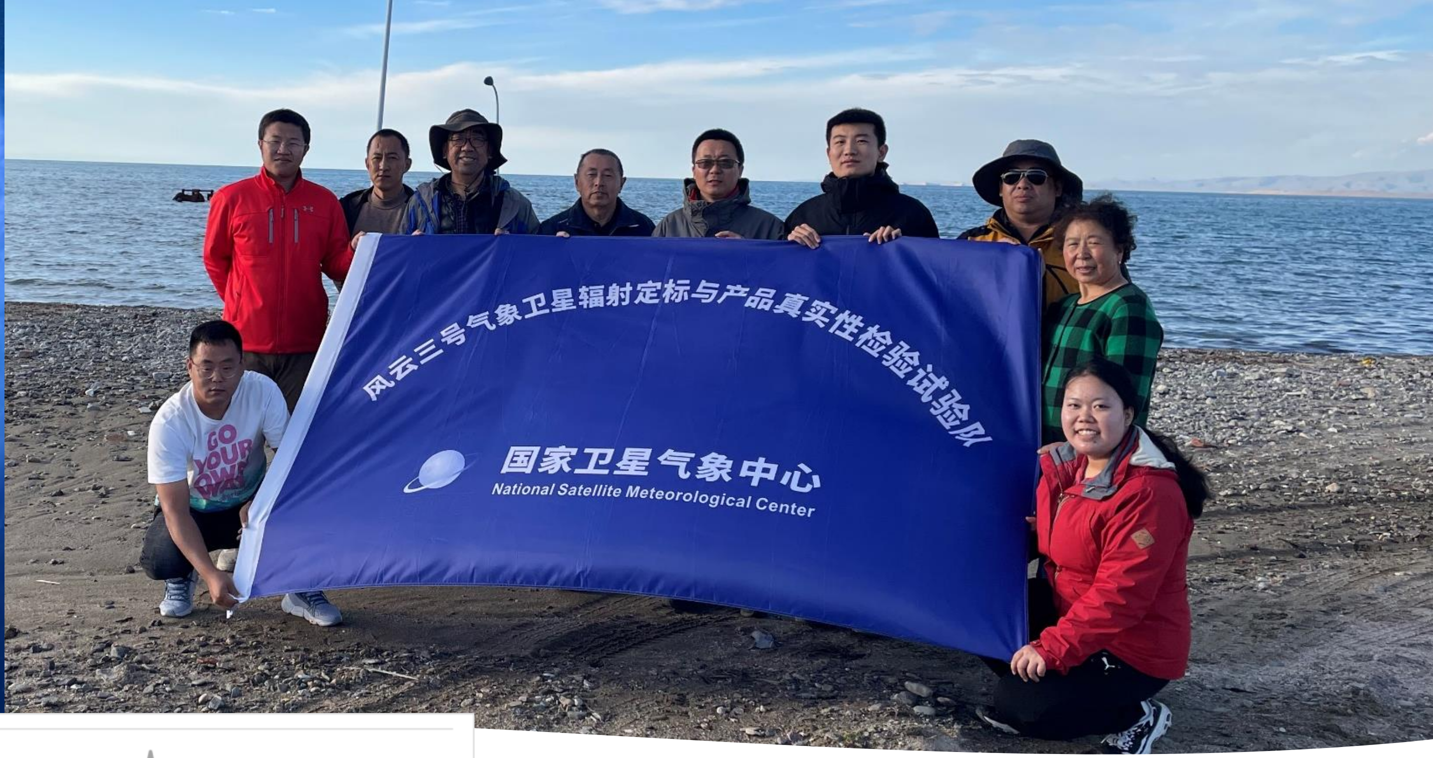

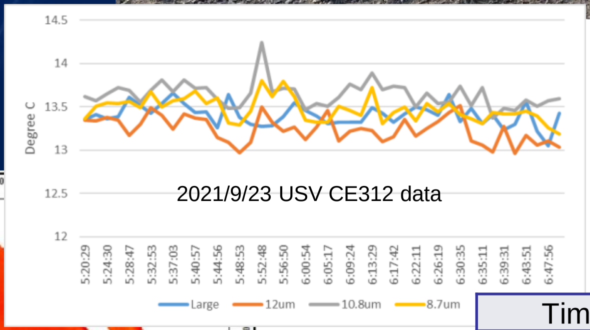

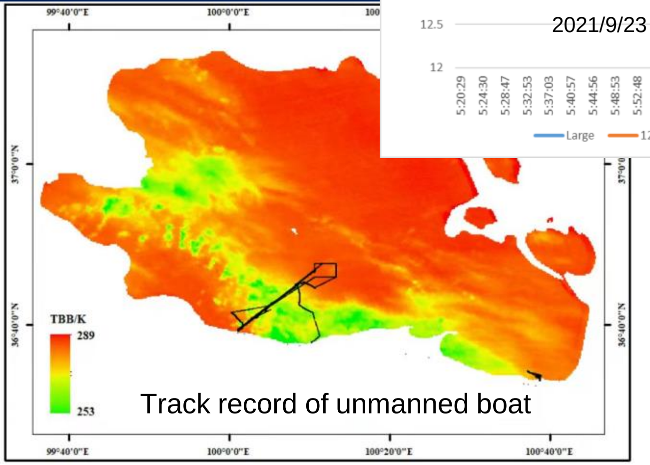

- Calibration evaluation preliminary results

Time	Sat	Band	Simulated BT	Observed BT	Diff
9.22 18:37	E	10.8um	285.1113094	285.768165	-0.65686
		12um	284.3188356	284.427184	-0.10835
9.23 6:58	E	10.8um	285.0539585	284.399176	0.654782
		12um	284.5785044	283.17882	1.399684
9.23 18:18	E	10.8um	285.6467885	284.895965	0.750824
		12um	285.2482131	283.568298	1.679915
9.21 14:36	D	10.8um	284.8564835	284.399176	0.457308
		12um	284.226621	283.646043	0.580578

Thanks for your attention!